

Fluctuations in Angular Distributions of $^{12}\text{C}(^{16}\text{O}, \alpha)^{24}\text{Mg}^\dagger$

M. L. HALBERT, F. E. DURHAM,* C. D. MOAK, AND A. ZUCKER

Oak Ridge National Laboratory, Oak Ridge, Tennessee

(Received 29 March 1967)

Angular distributions for a number of α -particle groups from $^{12}\text{C}(^{16}\text{O}, \alpha)^{24}\text{Mg}$ were measured with 45-keV resolution at closely spaced energies centered on bombarding energies of 19, 31, 42, and 49 MeV. Fluctuations of the type described by Ericson were observed. The data near 31 MeV were extensive enough to permit a statistical analysis. Compound levels with spins of about 10 are predominant at this energy. The average coherence width is about 125 keV and is independent of angle. No finer structure was found when the energy resolution was reduced to 15 keV. The strength of the fluctuations is generally in agreement with the expectation for a pure compound-nucleus process, though some anomalies were discovered. The coherence angle is about 6° , in agreement with expectation based on the size of the nucleus and the wave number. The angle-integrated average cross sections near 31 MeV are proportional to the statistical weights of the final levels.

I. INTRODUCTION

WE have made extensive studies of the reaction $^{12}\text{C}(^{16}\text{O}, \alpha)^{24}\text{Mg}$ with particular emphasis on the rapid fluctuations of the cross sections as a function of energy.^{1,2} As pointed out by Ericson,³ Brink and Stephen,⁴ and others, a statistical analysis of the fluctuations can yield important average properties of the participating compound states. Since the angular distributions are also expected to show fluctuation effects,^{3,5} detailed measurements of $d\sigma/d\Omega$ were made, and they are reported in this paper. Other experimenters have made measurements on this reaction.^{6,7,8}

Angular distributions were measured in four regions of bombarding energy near 19, 31, 42, and 49 MeV. These energies correspond approximately to 25-, 30-, 35-, and 38-MeV excitation energy in the ^{28}Si compound nucleus. Table I summarizes the experimental measurements. The most extensive data consist of 29 sets of angular distributions spaced, for the most part, at

100-keV intervals from 29.55 to 32.65 MeV (lab). Each set consists of data for the five groups α_0 , α_1 , $\alpha_2 + \alpha_3$, α_4 , and $\alpha_5 + \alpha_6$, corresponding to the ground state and first six excited levels of ^{24}Mg . The 100-keV spacing corresponds to 43 keV in the center-of-mass (c.m.) system; this is about one-third of the typical coherence width of the structure in the excitation functions. The energy resolution in the entrance channel was about 45 keV (c.m.). The data near 19 and 42 MeV comprise, respectively, six and three sets of angular distributions, also at 100-keV intervals. Near 49 MeV, data were obtained at only one energy.

The angular distributions are symmetric about 90° and exhibit rapid fluctuations with energy, as predicted by Ericson.³ Statistical analyses of the 31-MeV data, which cover an energy span of about $\sim 11\Gamma$, were carried out to extract the coherence angle, coherence energy, and nonfluctuating (direct-interaction) fraction of the cross section. Data at the other energies do not

TABLE I. Summary of angular-distribution measurements. Excitation energies in MeV and the spins and parities of the ^{24}Mg levels are listed below the symbol for each group.

Laboratory energies (MeV)	Center-of-mass energies (MeV)	^{28}Si excitation energies (MeV)	C.M. energy resolution (keV)	Groups studied						
				α_0 0 0+	α_1 1.37 2+	$\alpha_2 + \alpha_3$ 4.12 4.23 4+ 2+	α_4 5.22 3+	$\alpha_5 + \alpha_6$ 6.00 6.44 4+ 0+		
18.95-19.55	8.12-8.38	24.88-25.14	50	x	x					
29.55-32.65	12.66-13.99	29.42-30.75	45	x	x	x		x		x
41.55-41.95	17.81-17.98	34.56-34.74	40	x	x	x				
48.95	20.98	37.74	35	x	x	x				
18.40-19.00	7.89-8.14	24.64-24.90	15	x	x	x		x		
19.07-19.80	8.17-8.49	24.93-25.24	15	x	x	x		x		
29.85-30.30	12.80-12.99	29.55-29.74	15	x	x	x				

[†] Research sponsored by the U. S. Atomic Energy Commission under contract with the Union Carbide Corporation.

* Temporary employee from Tulane University; partial support received from Oak Ridge Associated Universities.

¹ M. L. Halbert, F. E. Durham, C. D. Moak, and A. Zucker, Nucl. Phys. **47**, 353 (1963).

² M. L. Halbert, F. E. Durham, and A. van der Woude, preceding paper, Phys. Rev. **162**, 899 (1967).

³ T. Ericson, Ann. Phys. (N. Y.) **23**, 390 (1963).

⁴ D. M. Brink and R. O. Stephen, Phys. Letters **5**, 77 (1963).

⁵ T. Ericson, Advan. Phys. **9**, 425 (1960).

⁶ A. R. Quinton and G. P. Lawrence, Phys. Letters **6**, 231 (1963).

⁷ D. E. Groce and G. P. Lawrence, Nucl. Phys. **67**, 277 (1963).

⁸ N. Drysdale, A. J. P. L. Policarpo, and W. R. Phillips, in *Comptes Rendus du Congrès International de Physique Nucléaire*, edited by P. Guenberger (Centre National de Recherche Scientifique, Paris, 1964), Vol. II, p. 706.

cover a sufficient range of energies for meaningful statistical analysis, but certain interesting features will be discussed.

Portions of the measurements were repeated with a much thinner target to check for narrower structure.

II. EXPERIMENTAL DETAILS

The measurements were made with basically the same equipment used for the excitation functions,^{1,2} but there were many differences in detail. The following description emphasizes the significant differences.

Nine silicon surface-barrier detectors were used simultaneously, as shown in Fig. 1. One of these was fixed at about 14° to serve as a monitor. The other eight were mounted on a base plate which could be rotated about the target, located at the center of the reaction chamber. Four detectors were spaced at 20.0° intervals in the forward direction, while the others were placed at 20.0° intervals directly opposite the first four. Normal operating procedure consisted of making eight successive runs at a given energy, with the base plate moved 2.5° after each run. The runs were made with counter 1 at angles of 12.5° , 15.0° , \dots , 30.0° to the beam direction. In this way 64 angles were measured from 12.5° to 167.5° , at 2.5° intervals. The c.m. acceptance of all counters was a cone of half angle approximately 2° .

Particles emitted at 90° were detected by both counter 4 and counter 5 when counter 1 was at 30° . Since the α yields vary rapidly with angle, this duplication enabled us to determine the beam direction to 0.1° by matching the relative counting rates in detectors 4 and 5 for different α groups.

The signals from the eight movable detectors were amplified by eight high-gain low-noise preamplifiers connected to the eight inputs of an 800-channel pulse-height analyzer operated in 100-channel subgroups. The monitor signals were amplified and sent to a single-channel discriminator with its window centered on the peak due to elastic scattering of ^{16}O by ^{12}C . The length of each run was governed by the number of counts from this discriminator. The integral of the beam current

passing through the target to the Faraday cup was also recorded for each run.

Buildup of carbon on the targets was noted during these runs despite the use of a liquid-nitrogen-cooled shield around the target. Earlier indications¹ that this shield eliminated the buildup were not borne out in the present work, although some reduction in the rate of buildup was noticed. The buildup had no effect on the accuracy of the cross sections because the monitor counter was used to determine the length of each run. To maintain a sharp entrance-channel energy resolution, however, it was necessary to watch the increase in target thickness carefully. When the integrated beam current for a fixed monitor count showed that an increase of about 20% in the target thickness had occurred, the target was moved to expose a fresh spot to the beam.

To prevent the side of the target holder from intercepting the emitted α particles, the targets were tilted so that the normal to the target made an angle of $\sim 35^\circ$ with the beam direction, as shown in Fig. 1. The effective target thicknesses were combined with the energy loss in carbon given by Northcliffe⁹ to obtain the effective c.m. energy resolutions indicated in Table I.

For the special thin-target measurements, carbon films of $3.3 \mu\text{g}/\text{cm}^2$ (as estimated from their optical density) were placed perpendicular to the beam direction. The over-all energy resolution for these runs is estimated at $\sim 15 \text{ keV}$ (c.m.).

The absolute cross sections for the 19- and 31-MeV data were calculated from the elastic scattering counting rate in the monitor at 14° lab ($\sim 33^\circ$ c.m.) since the scattering at 19 MeV is known to follow the Rutherford law for angles as large as 42° c.m.¹⁰ As a check, some of the 19-MeV cross sections for the $^{12}\text{C}(^{16}\text{O},\alpha)$ reaction were calculated directly from the integrated beam current, solid angle, and estimated target thickness; the agreement was satisfactory. The absolute cross sections near 19 MeV are believed to be reliable to about $\pm 15\%$. Where a cross section is unusually small, the statistical uncertainty in the number of counts becomes significant. For most of the data, 1 mb/sr corresponds to roughly 2000 counts. Thus, cross sections below 0.01 mb/sr are uncertain by more than 20% because of counting statistics. An uncertainty this large occurs only rarely.

For the 31-MeV data, the elastic counting rate relative to that at 19 MeV was determined for the monitor counter for fixed integrated beam current in the Faraday cup. A correction was necessary because the average charge of the ^{16}O ions due to stripping of electrons as they passed through the target is different for the two beam energies. At 29.6 MeV the change in average charge was measured by alternately inserting and with-

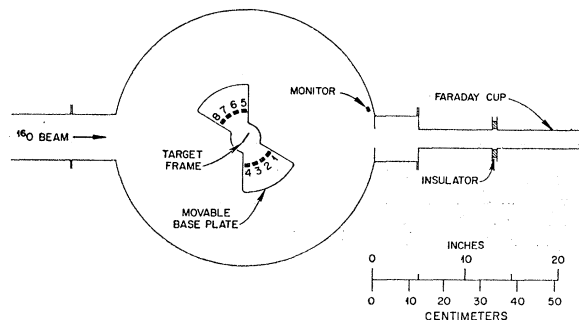


FIG. 1. Experimental arrangement. The base plate is shown with counter 1 at 30° . The angle accepted by the detectors is not shown in correct scale.

⁹ L. C. Northcliffe, *Ann. Rev. Nucl. Sci.* **13**, 69 (1963).

¹⁰ D. A. Bromley, J. A. Kuehner, and E. Almquist, *Reactions between Complex Nuclei*, edited by A. Zucker, F. T. Howard, and E. C. Halbert (John Wiley & Sons, Inc., New York, 1960), p. 151.

drawing the target carrier while the accelerator was operating steadily. The average charge with the target in was 7.16 ± 0.14 . The 19.0-MeV average charge was taken as 6.47, interpolated from similar measurements at 17.6 MeV (6.40 ± 0.11) and at 20.7 MeV (6.56 ± 0.07).

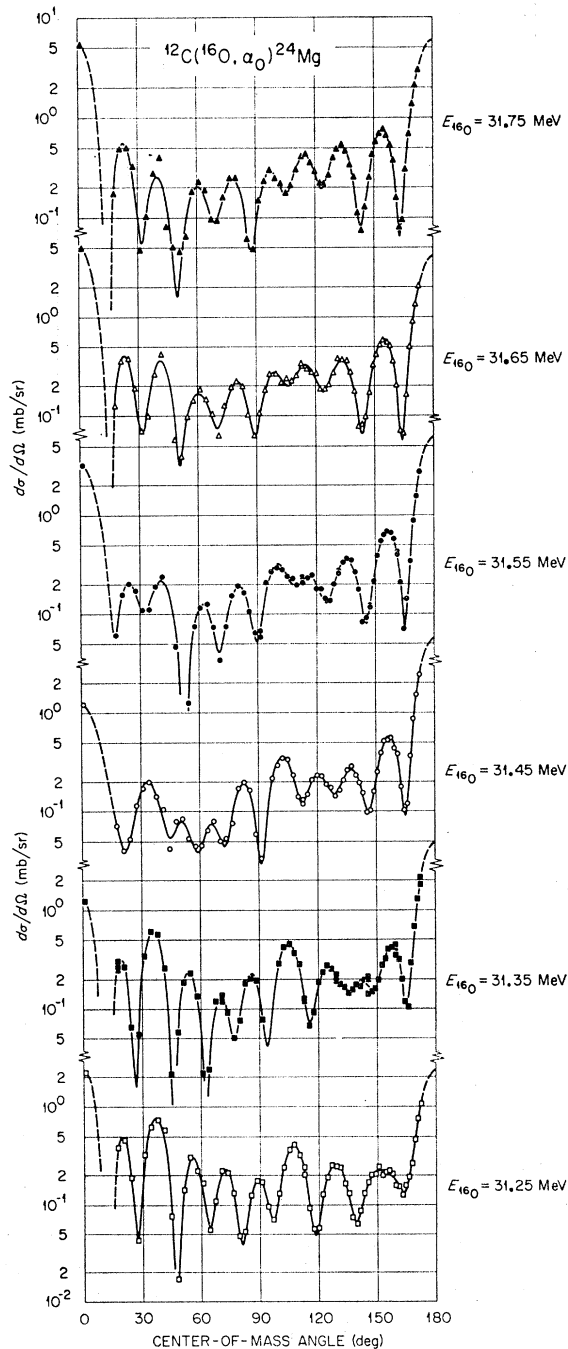


FIG. 2. Angular distributions for $^{12}\text{C}(^{16}\text{O}, \alpha)^{24}\text{Mg}$ at bombarding energies from 31.25 to 31.75 MeV. The points are experimental measurements, while the curves are least-square fits with sums of Legendre polynomials to order 24. Dashed portions indicate regions where no data were obtained.

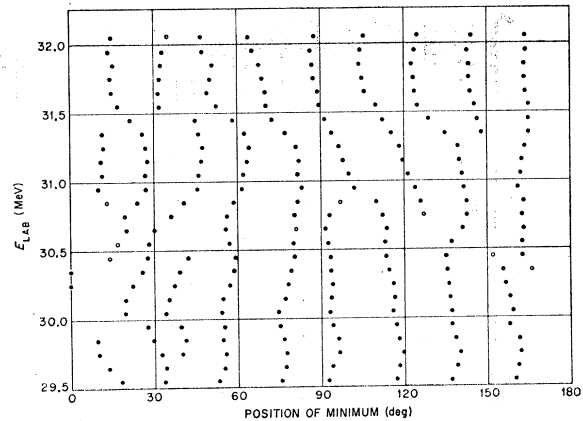


FIG. 3. Positions of minima in the least-square fits to the ground-state angular distributions near 31-MeV bombarding energy. Open circles indicate points of inflection.

These values are within a few percent of the average charge calculated from the equilibrium charge distributions of heavy ions in low- Z materials.⁹ The reliability of the absolute cross sections near 31 MeV is also estimated to be about $\pm 15\%$, except that the α_4 and $\alpha_5 + \alpha_6$ results are subject to additional uncertainties because of background and resolution problems, particularly where the cross sections for these two groups are small.

The 42- and 49-MeV data had to be treated differently because no measurement was made of the elastic counting rate relative to the 19-MeV rate. The absolute cross sections were calculated from the estimated target thickness, integrated beam current, solid angle, and average charge, the latter being calculated from the equilibrium charge distributions.⁹ Largely because of the uncertainty in target thickness, the cross-section scale for the 42- and 49-MeV is estimated to be uncertain by about $\pm 25\%$.

At three energies (29.55, 30.55, and 31.55 MeV), additional data were obtained at angles from 0° to 10.0° in 2.5° steps. The method of stopping and monitoring the beam is described in Ref. 2.

Although the 100-keV spacing of the 31-MeV measurements was known quite accurately, the entire bombarding energy scale is uncertain² by about 100 keV. The energies quoted take into account the energy loss of the beam in the target, and correspond always to mean bombarding energies.

III. RESULTS

All differential cross sections are given in the c.m. system.

31-MeV data. A sample of the angular distributions for the α_0 group is shown in Fig. 2. The points at 1.5° are from the "zero-degree" data of Ref. 2. Rapid fluctuations are evident. For example, between 31.45 and 31.55 MeV (a change of only 43 keV c.m.), the maximum at 35° changes to a minimum. The positions of the other maxima and minima also change rapidly

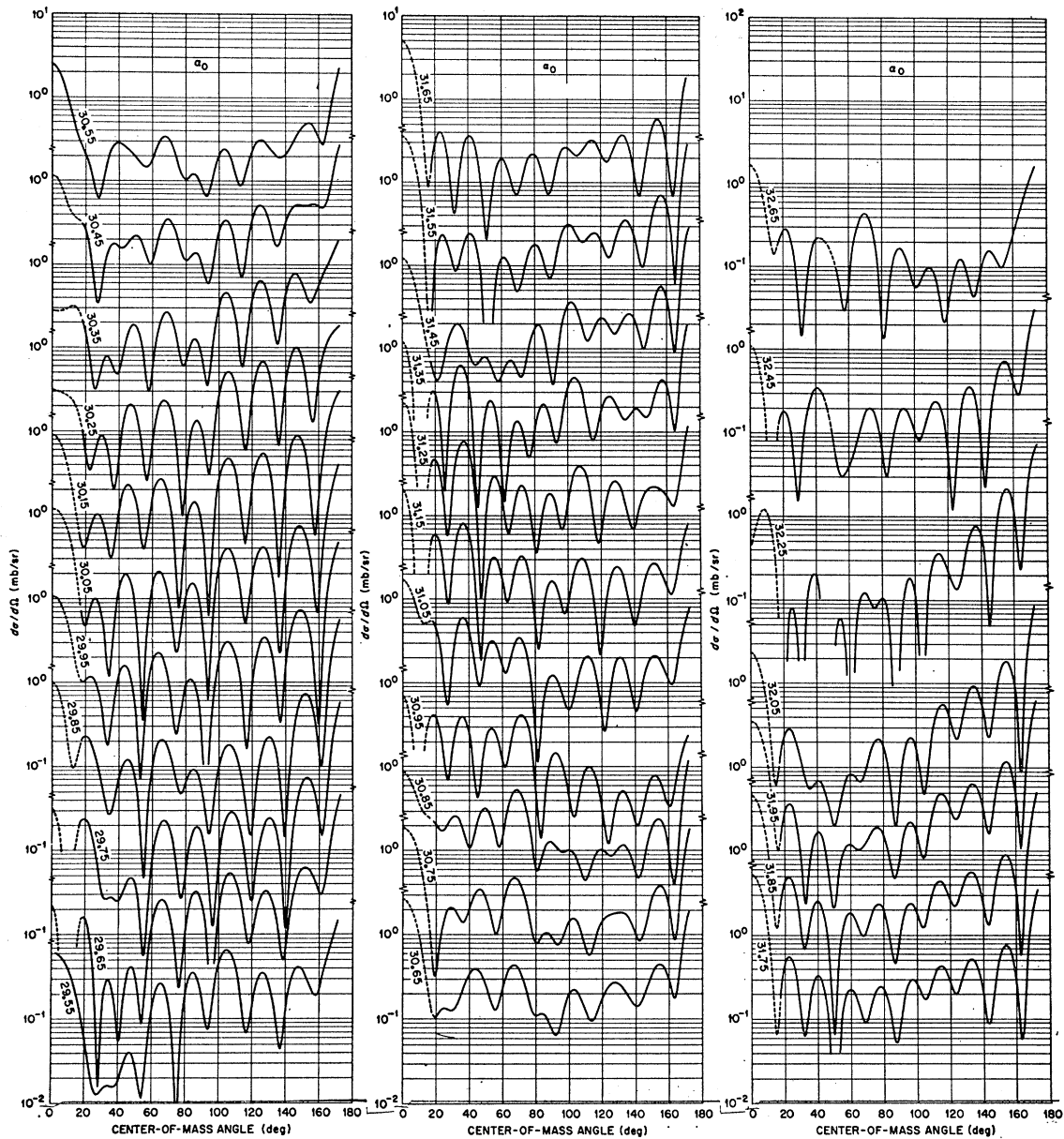


FIG. 4. Least-square fits with Legendre polynomials to order 24 for the α_0 angular distributions near 31-MeV bombarding energy. Dashed portions of the curves represent regions where no experimental data were obtained.

and in irregular fashion. These shifts in angle are far too rapid to be the variation with energy of a diffraction pattern. Moreover, the shifts are not monotonic, as shown in Fig. 3, which is a plot of the positions of the minima in the α_0 angular distributions as a function of energy.

The smooth curves in Fig. 2 are least-square fits to sums of Legendre polynomials. That is, the cross section is expressed as

$$\frac{d\sigma}{d\Omega} = \sum_{k=0}^K B_k P_k(\cos\theta). \quad (1)$$

The fits were made with $K=24$. Figures 4 to 8 show the fits for the 29 angular distributions obtained for each α -particle group from 29.55 to 32.65 MeV.

A check of the α_0 , α_1 , $\alpha_2+\alpha_3$, and α_4 cross sections at two energies showed that these results agree within 10–20% with our 30° and 148° (lab) excitation functions reported earlier.¹ In making this comparison, it was necessary to shift the earlier data downward by 150 keV (lab). One-third of this energy shift is required to allow for energy loss of the beam in the target, which was not included in the previously pub-

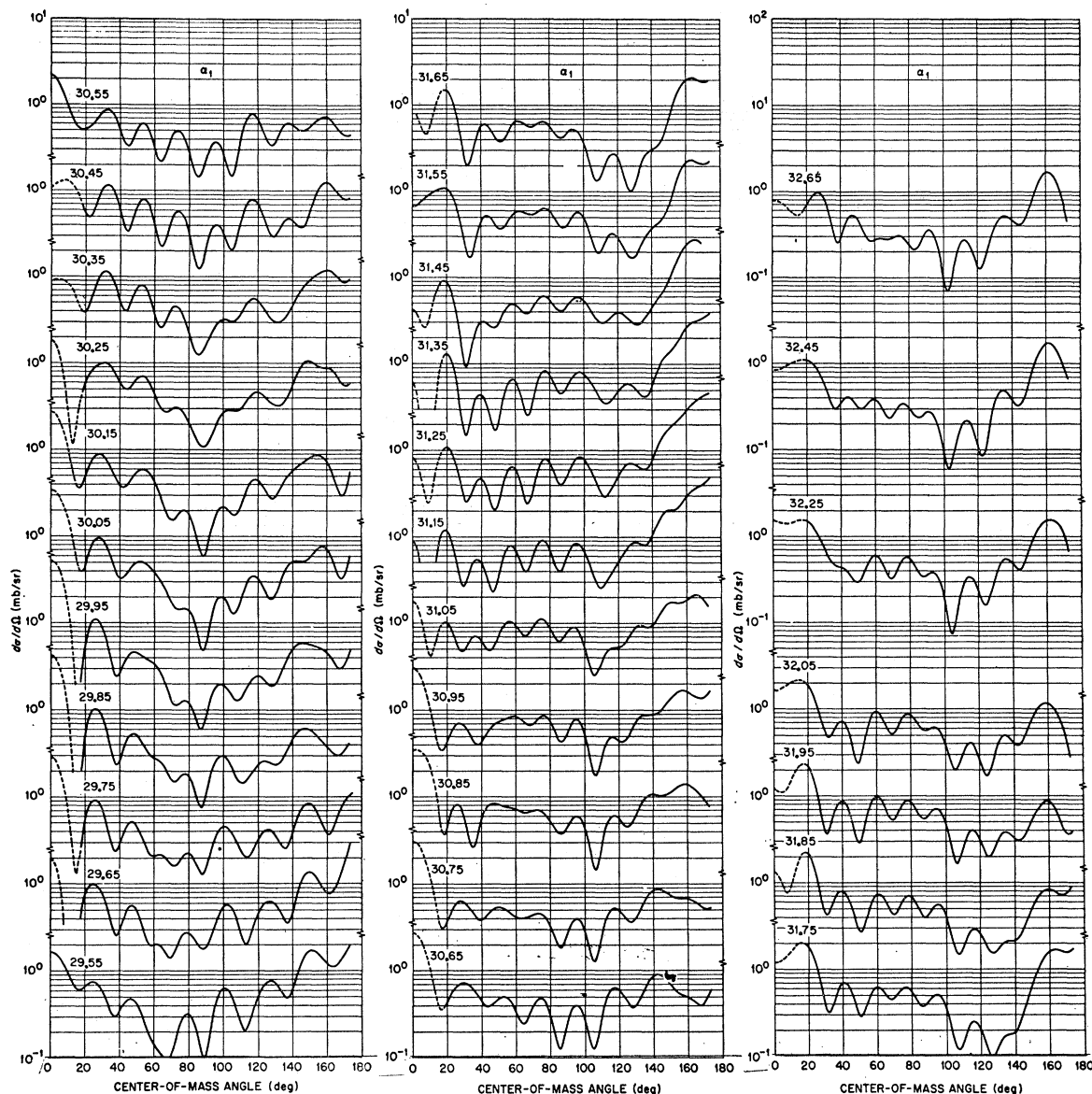


FIG. 5. Least-square fits with Legendre polynomials to order 24 for the α_1 angular distributions near 31-MeV bombarding energy. Dashed portions of the curves represent regions where no experimental data were obtained.

lished results.¹ The other 100-keV shift is within the estimated uncertainty of the beam energy.

Another comparison is possible. A portion of the differential cross section for α_0 at about 31.9 MeV was measured by Quinton and Lawrence.⁶ Again, allowing for energy loss in their target and a 100-keV uncertainty in our bombarding energy, the corresponding data from Fig. 4 are in substantial agreement.

The orbital angular momentum involved in the reaction cannot be much higher than kR in the entrance channel. With an interaction radius of $R=1.2[(12)^{1/3} + (16)^{1/3}]$ F, the value of kR is 12.08 for 31.15 MeV, the bombarding energy at the midpoint of the 29.55–32.65-MeV interval. Thus, partial waves with $l > 12$ are not

expected to play any important role. A check can be obtained from the least-square fits to (1) since the order of the highest Legendre polynomial required for an adequate fit to the data is twice the highest l value involved. For these data, the highest k values for which B_k was significantly different from zero were 20 to 24, indicating that partial waves above $l=10$ to 12 are not important. Tests were made with $K=26$ in (1); the fits did not improve and the B_k were practically unchanged. On the other hand, the pronounced structure showing 7 to 9 minima suggests that the low- l partial waves are also small.

Partial-wave analyses were attempted by an iterative least-squares procedure with the hope of verifying these

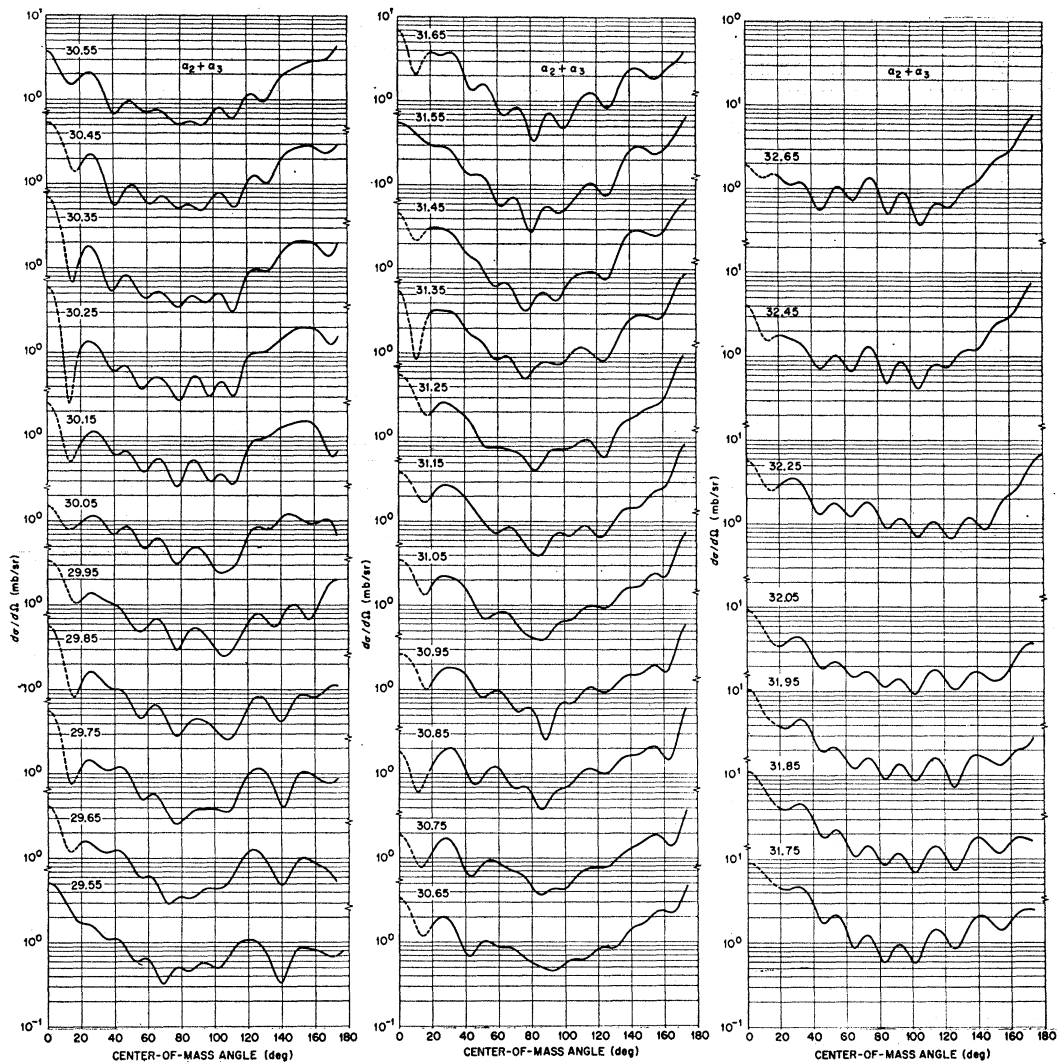


Fig. 6. Least-square fits with Legendre polynomials to order 24 for the $\alpha_2 + \alpha_3$ angular distributions near 31-MeV bombarding energy. Dashed portions of the curves represent regions where no experimental data were obtained.

inferences and of tracing the energy dependence of the partial-wave amplitudes. A large number of solutions exist which give identical fits to the data.¹¹ It was hoped at first that only one, or at most a few, would be physically reasonable, but every one of the dozen or so solutions found in preliminary tests by random choice of the initial amplitudes was physically acceptable. Moreover, the iteration process proved to be unstable when applied to this problem. Extremely wild excursions were usual during the early iterations and the converged solutions bore no resemblance to the starting parameters, so that the energy variation of a particular partial-wave amplitude could not be studied. For these reasons the partial-wave analysis was abandoned.

¹¹ J. A. Kuehner, J. D. Prentice, and E. Almqvist, Phys. Letters 4, 332 (1963).

Calculations of cross sections for 31.3-MeV bombarding energy were done at Chalk River using the statistical compound-nucleus theory.¹² Figure 9 shows the calculated contributions to the angle-integrated α_0 cross section from compound states of various spin values. The $J=8$ to $J=12$ region is dominant, and contributes almost 80% of the cross section. Since the final particles have zero spin, we expect that the partial waves near $l=10$ should likewise dominate the angular distribution, in agreement with the experimental results.

The angle-integrated cross section σ_T can be obtained easily from the fit to Eq. (1); it is simply $4\pi B_0$. Figure 10 shows this quantity as a function of energy for all the data. A problem was encountered for $\alpha_5 + \alpha_6$. The experimental data extended only to about 155° because

¹² E. Vogt and D. McPherson (private communication).

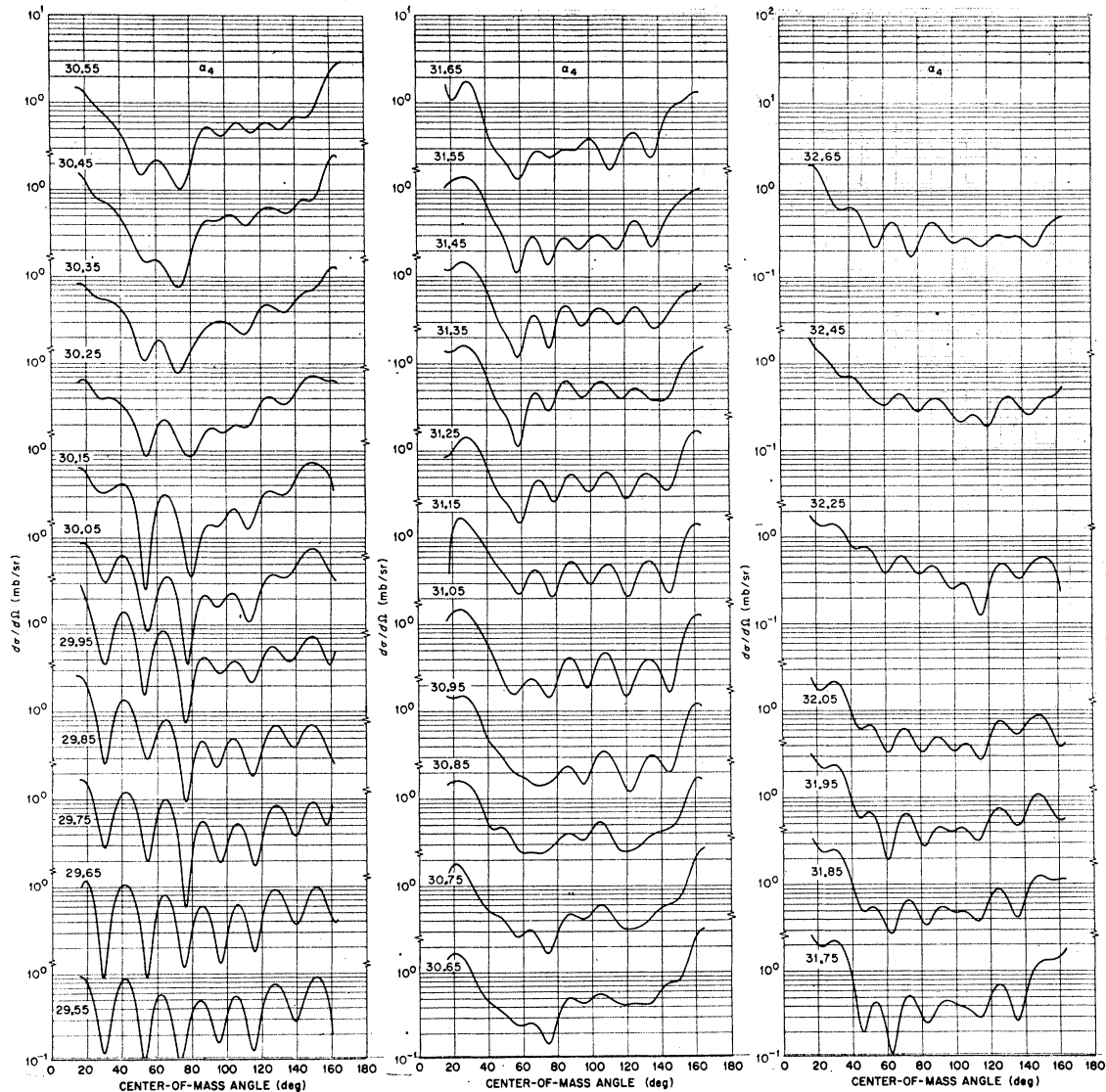


FIG. 7. Least-square fits with Legendre polynomials to order 24 for the α_4 angular distributions near 31-MeV bombarding energy.

these particles have very low energy at extreme back angles. At some energies the least-square fits behaved unreasonably (e.g., negative cross sections beyond 155°) and the uncertainty in B_0 was comparable with its magnitude. Both of these problems could be eliminated by supplying an estimate of the 180° (and/or 170°) cross section. The magnitude of B_0 was insensitive to these estimates. For example, when the 180° cross section was increased from 0.001 to 10.0 mb/sr, B_0 increased by only 15% at 30.15 MeV and 10% at 32.45 MeV. The values of σ_T for $\alpha_5 + \alpha_6$ that are shown in Fig. 10 were obtained with intermediate estimates, and are therefore uncertain on this account by 10 or 20%. Although the α_4 angular distributions also do not include data at extreme back angles, the problems just discussed do not arise. The 0° and 180° cross sections

are known to be zero since the fourth excited state of $^{24}\text{Mg}(3^+)$ has unnatural parity.¹⁸ When these zero cross sections were included in the data to be fitted, the least-square fits for α_4 were found to be well behaved.

19-MeV Data. Differential cross sections were obtained for the α_0 and α_1 groups at six energies, 18.95, 19.05, ..., and 19.45 MeV. The experimental results for 18.95 MeV are shown as points in Fig. 11. For simplicity, the data points at the other energies are not shown since the least-square fits give an adequate representation. More than 64 points are shown for 18.95 MeV; the extra data were taken for determination of relative solid angles. The smooth curves are least-square fits to expression (1) with $K=12$. It was

¹⁸ A. E. Litherland, Can. J. Phys. 39, 1245 (1961).

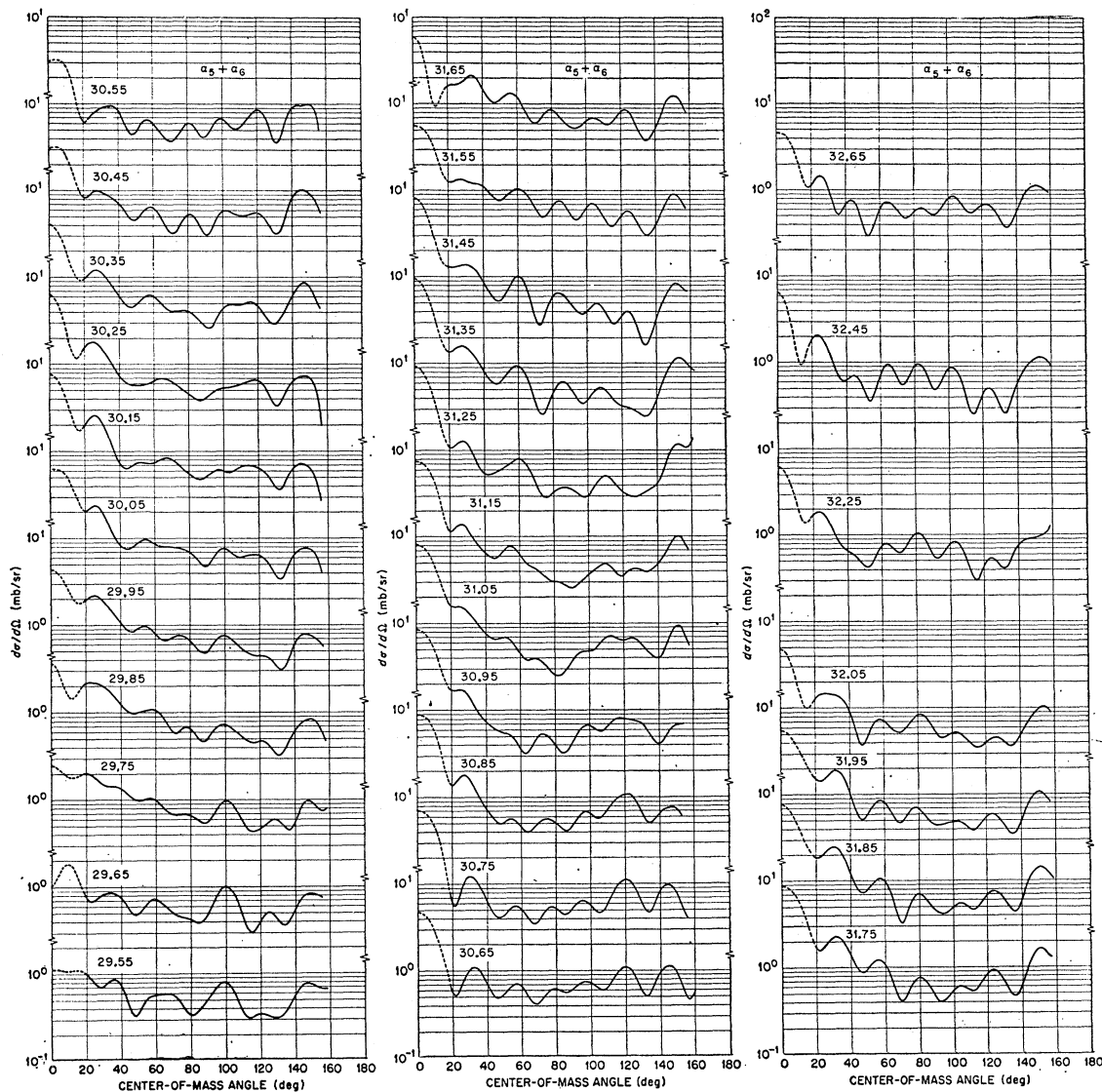


FIG. 8. Least-square fits with Legendre polynomials to order 24 for the $\alpha_5 + \alpha_6$ angular distributions near 31-MeV bombarding energy. Dashed portions of the curves represent regions where no experimental data were obtained.

found that usually B_{10} is the highest coefficient making a significant contribution, so that the highest partial waves involved are those with $l=5$. Figure 10 contains the values of $4\pi B_0$ from these fits.

As before, these results agree well with our previously published¹ excitation functions at 30° and 149° (lab) provided that an appropriate small adjustment of the energy scale is made. However, a problem appears when these results are compared with those of Ref. 7 in the 500-keV region common to both measurements. The ratio of the α_0 and α_1 angle-integrated cross sections reported in Ref. 7 is in good agreement with our results, again provided that we allow for a shift in the energy scale due in part to the absence of a target-

thickness correction in Ref. 7. But our absolute cross sections are nine times smaller, and a similar discrepancy is evident in the differential cross sections. The sum of the angle-integrated cross sections of Ref. 7 for α_0 through α_6 is about 250 mb at 9.5 MeV (c.m.). Since this energy is very close to the entrance-channel Coulomb barrier, the total reaction cross section should be on the order of half of the geometric cross section; the latter is about 1.6 b. It seems unlikely that the cross section for only seven α groups could amount to 30% of the total cross section. Thus, we believe that the results of Ref. 7 are too large by an order of magnitude.

42-MeV data. The α_0 , α_1 , and $\alpha_2 + \alpha_3$ cross sections are presented in the lower part of Fig. 12 for three energies near 42 MeV. Experimental points are given

only for 41.75-MeV mean bombarding energy. The increase in the number of minima shows that higher partial waves are now important. The least-square fits were made with $K=28$. A test was made with $K=32$ for the α_0 data. The coefficients B_{28} through B_{32} were found to be much smaller than B_0 through B_{27} , and were not statistically different from zero. This indicates that partial waves above $l=13$ or 14 are probably not contributing significantly, in agreement with predictions of the statistical model.¹² The angle-integrated cross sections are shown in Fig. 10.

49-MeV data. The cross sections for α_0 , α_1 , and $\alpha_2+\alpha_3$ at 48.95-MeV mean energy in the target are several times smaller than at 42 MeV, particularly for α_0 (about five times weaker). The angular distributions are shown in the upper part of Fig. 12 together with least-square fits for $K=32$. The mediocre fit with the α_0 data is probably due to poor counting statistics. The integrated cross sections are given in Fig. 10.

Thin-target data. Excitation functions for α_0 , α_1 , and $\alpha_2+\alpha_3$ near 19 and 30 MeV were remeasured with a resolution estimated at 15 keV (c.m.). Data were obtained simultaneously at angles of 30° , 50° , 70° , 110° , 130° , and 150° (lab). In no case could structure finer than 100 keV be discerned. Figure 13 shows comparisons between two samples of these data and excitation functions constructed from the data of Figs. 4 and 6.

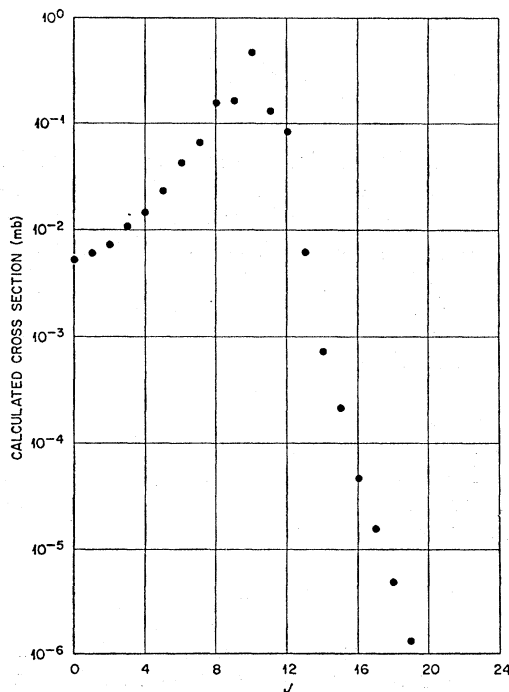


FIG. 9. Contributions to the angle-integrated α_0 cross section as a function of compound-state spin for an average bombarding energy of 31.1 MeV, according to a statistical-model calculation (Ref. 12).

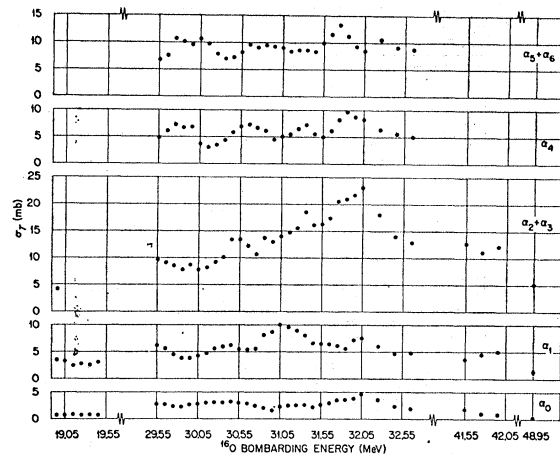


FIG. 10. Angle-integrated cross sections obtained from the least-square fits of the differential cross sections as a function of the mean ^{16}O bombarding energy in the target.

IV. ANALYSIS OF FLUCTUATIONS

The data covering the widest span of energies (1.33-MeV c.m.) were those near 31 MeV. Statistical analysis of the fluctuations was carried out to obtain the coherence angle, the autocorrelation $R(0)$, and the average compound-nucleus width Γ . Because of the relatively small sample size, $\sim 11\Gamma$, biases and statistical uncertainties due to finite-sample effects are appreciable. A full account of the theoretical considerations for $R(0)$ and Γ and the relevant sample-size corrections, according to the Ericson and Brink-Stephen simplified model of the compound nucleus, is given in Sec. IV and Appendix B of the preceding paper.² The formulas from Ref. 2 used in the present calculations will be identified in the appropriate places.

A. Coherence Angle

Fluctuations at neighboring angles are correlated, but cross sections at widely separated angles are statistically independent. The coherence angle over which correlations exist is obtained from the characteristic width of the angular cross-correlation function as a function of β , the difference between any pair of angles. This function is defined by

$$R_\theta(\beta) = \frac{\langle \sigma(E, \theta) \sigma(E, \theta + \beta) \rangle}{\langle \sigma(E, \theta) \rangle \langle \sigma(E, \theta + \beta) \rangle} - 1, \quad (2)$$

where the brackets denote averages over E , the energy. Brink, Stephen, and Tanner¹⁴ have shown that $R_\theta(\beta)$ should resemble a diffraction pattern as a function of β with a width of the order of $(kR)^{-1}$. The detailed de-

¹⁴ D. M. Brink, R. O. Stephen, and N. W. Tanner, Nucl. Phys. **54**, 575 (1964).

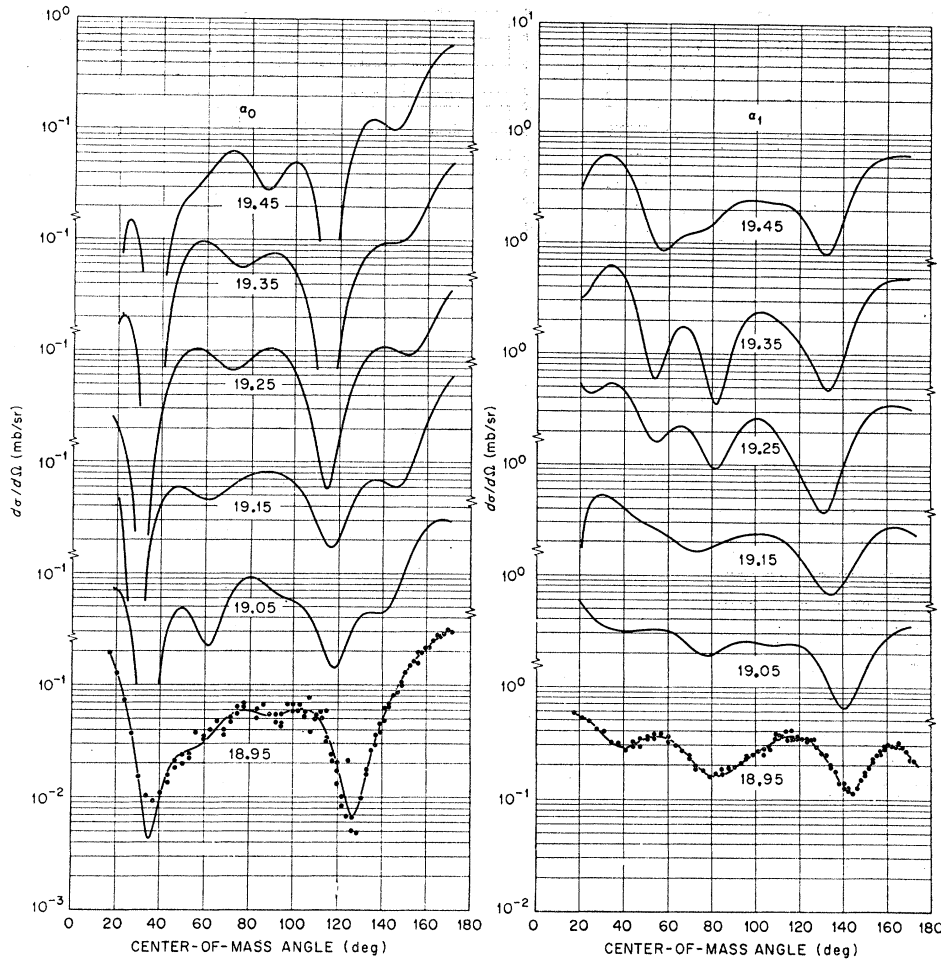


FIG. 11. Angular distributions near 19-MeV bombarding energy. Experimental points are shown for 18.95 MeV only. The smooth curves are least-square fits with sums of Legendre polynomials up to order 12.

pendence on β depends on the particular nuclear model chosen. For a surface-emitting sphere of radius R , the theoretical prediction is¹⁴

$$R_{\theta}(\beta) = [(\sin kR\beta)/kR\beta]^2. \quad (3)$$

The half-width at half-maximum of this function is given by $1.39/(kR)$, which is 6.6° for the present case.

We did not make a detailed examination of $R_{\theta}(\beta)$ for all 64 values of θ . Instead, we averaged over θ in order to show the over-all trends clearly. We will designate the average of $R_{\theta}(\beta)$ over all angles θ by $R_{av}(\beta)$. The cross sections were measured at angles spaced equally in the laboratory system, but these correspond to grossly unequal β in the c.m. system, so that it is impossible to calculate $R_{av}(\beta)$ directly from the experimental cross sections. Therefore, $R_{av}(\beta)$ was calculated by using the Legendre-polynomial least-square fits. The results are shown in Fig. 14 for all five α -particle groups.

We define the coherence angle as the half-width $\beta_{1/2}$ of these curves by the expression

$$R_{av}(\beta_{1/2}) = \frac{1}{2}[R_{av}(\beta_m) - R_{av}(0)], \quad (4)$$

where β_m is the location of the first minimum (or, for those curves without a clearcut minimum, the smallest $\beta > 0$ for which the slope is zero). We obtain the values $\beta_{1/2} = 4.7^\circ, 6.2^\circ, 6.6^\circ, 6.5^\circ,$ and 7.0° for $\alpha_0, \alpha_1, \alpha_2 + \alpha_3, \alpha_4,$ and $\alpha_5 + \alpha_6$, respectively; the average of these numbers is 6.2° , which corresponds to $kR = 12.86$. These results are in satisfactory agreement with the value expected for the model mentioned above.

Many of the curves, particularly the one for α_0 , show a diffraction-like structure with a spacing of 18° to 19° . According to the model, minima should occur at intervals of π/kR , or 14.9° for $kR = 12.08$. Although this discrepancy is not serious, it indicates that the model is probably oversimplified.

B. $R(0)$ for Differential Cross Sections

The autocorrelation function for $\epsilon = 0$ is of great interest because its expectation value $\bar{R}(0)$, depends on the number N of independently fluctuating channels, and on y , the ratio of the nonfluctuating (direct-interaction) cross section to the average cross section. The estimated N values² for all five groups are listed in Table II.

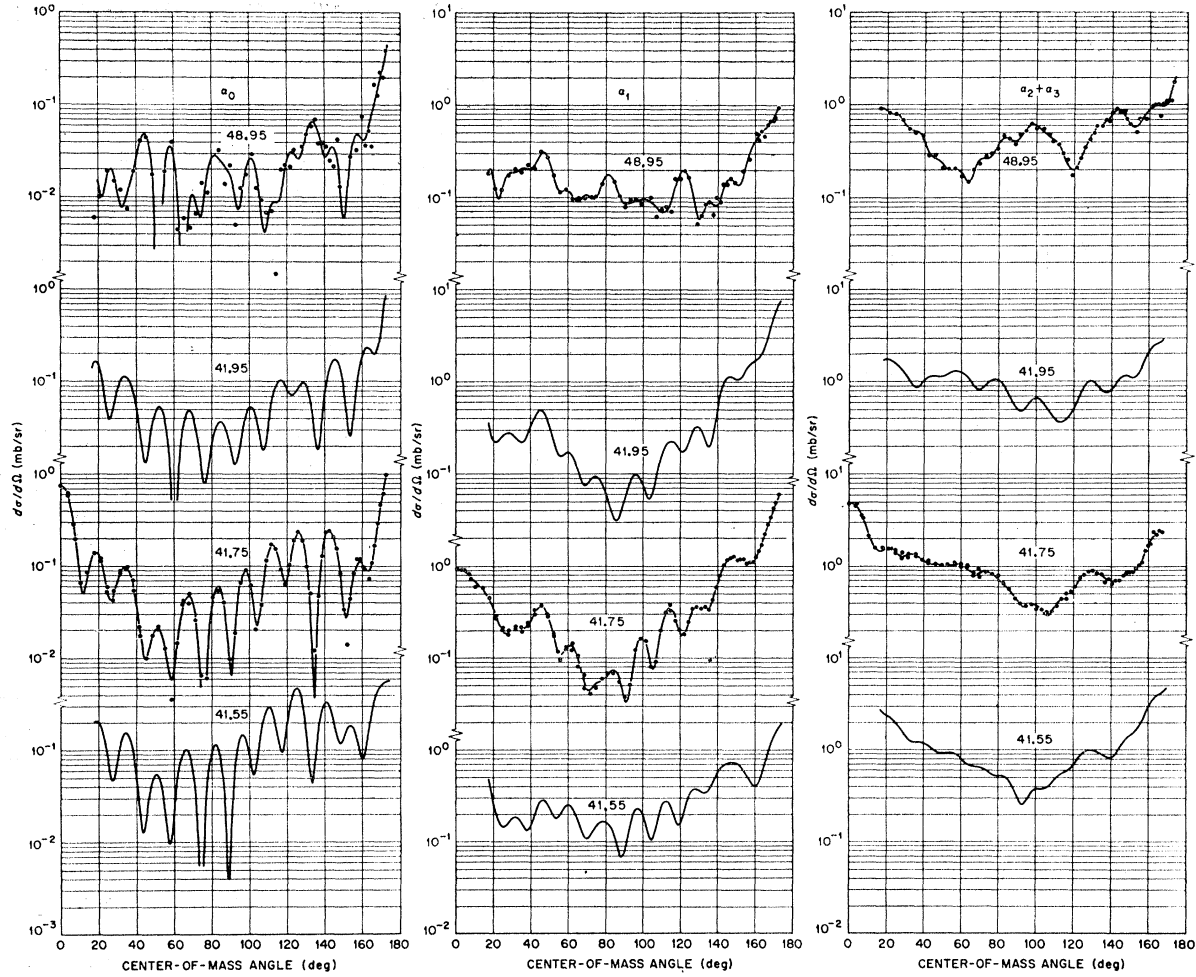


FIG. 12. Angular distributions near 42- and 49-MeV bombarding energy. Experimental points are shown for 41.75 and 48.95 MeV only. The smooth curves are fits with sums of Legendre polynomials to order 28 for the 42-MeV data and order 32 for the 49-MeV data.

For finite samples consisting of n statistically independent observations, $\bar{R}(0)$ is smaller than for infinite samples. In this work we use Eq. (B7) of Ref. 2 to obtain $\bar{R}(0)$. The 31-MeV data cover an interval of about 11Γ (if we assume $\Gamma \approx 115$ keV), so that the sample size n is about 4.7, according to Eq. (1) of Ref. 2. Thus finite-sample effects will be considerable. For example, for $N=1$ and no direct interaction ($y=0$),

$\bar{R}(0) = 0.65$. This may be compared with 1.00, the value expected in the absence of finite-sample effects.

In examining experimental results, it is necessary to know not only the expectation value but also the anticipated spread about the expectation value. For the α_0 data, the standard deviation of $R(0)$ about the expectation value of 0.65 is expected to be 0.42 for $y=0$, according to Eq. (B10) of Ref. 2. Figure 15 shows $R(0)$

TABLE II. Angle-averaged values of $R(0)$ for the differential cross sections, in comparison with $y=0$ predictions. The estimate of N the effective number of independently fluctuating channels, is for angles far from 0° or 180° . The quantity Q is the deviation of the experimental value from the expectation value, in units of the standard deviation, as defined in Eq. (5).

Group	Estimated		Experiment	$R(0)$		Q
	N	Region of averaging		Expectation		
α_0	1	$17^\circ-172^\circ$	0.508	0.648 ± 0.169	-0.82	
α_1	3	$30^\circ-150^\circ$	0.210	0.245 ± 0.059	-0.59	
$\alpha_2 + \alpha_3$	8	$30^\circ-150^\circ$	0.177	0.096 ± 0.021	+3.81	
α_4	3	$30^\circ-150^\circ$	0.174	0.245 ± 0.059	-1.19	
$\alpha_5 + \alpha_6$	6	$30^\circ-150^\circ$	0.084	0.127 ± 0.029	-1.48	

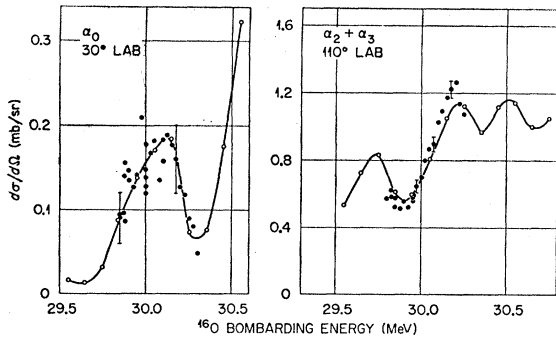


FIG. 13. Effect of improved energy resolution on excitation functions near 30 MeV. The solid points were obtained with a target thickness equivalent to 15 keV (c.m.), while the open circles are from data taken with 40–50-keV resolution. Typical counting statistics for the thin-target data are indicated by the error flags.

for α_0 as a function of angle; most of the values of $R(0)$ lie within the expected range. Incidentally, note that the characteristic widths of the structure in Fig. 15 are consistent with the coherence angles obtained in Sec. 1.

A better test of whether these results are consistent with the $y=0$ expectation value can be made by combining the data at different angles to obtain a result with less uncertainty. Suppose we combine i independent pieces of data to obtain the angle-average autocorrelation. According to the central-limit theorem, the expectation value of the angle average remains equal to $\bar{R}(0)$. Its distribution about $\bar{R}(0)$ tends to become Gaussian as i increases, with a variance $1/i$ times the variance of an individual measurement. We estimate i by expressing the angular span in terms of the coherence angle $\beta_{1/2}$. We assume that cross sections are substantially uncorrelated if they are separated by more than twice the full width of the angular cross-correlation function, that is, by more than $4\beta_{1/2}$. The α_0 data

covering angles from 17° to 172° is thus equivalent to $i \approx 6.25$ independent pieces of data, so that the expected standard deviation is $0.42/\sqrt{6.25} = 0.17$. The experimental angle-averaged value of $R(0)$ is 0.51; this is 0.8 standard deviation below the $y=0$ expectation, $\bar{R}(0) = 0.65$. Although the existence of a small nonfluctuating component cannot be ruled out, we may conclude that the data do not demand the presence of any direct interaction.

In applying this type of analysis to the other α groups, the regions near 0° and 180° must be kept separate from the intermediate angles because of the variation of N with angle.² In the α_1 data shown in Fig. 15, the values of $R(0)$ near 0° and 180° are consistent with $\bar{R}(0) = 0.65 \pm 0.42$, the expectation for $N=1$. At intermediate angles, we have $N=3$ and $\bar{R}(0) = 0.24$. We exclude the transition region from $N=1$ to $N=3$ by averaging $R(0)$ only from 30° to 150° ; the experimental angle-averaged value of $R(0)$ is 0.21. The standard deviation expected for the angle average of $R(0)$ over this range is 0.06; the experimental value of 0.21 is in agreement with the $y=0$ expectation of 0.24. Thus, the α_1 cross sections also do not demand any nonfluctuating component.

Table II lists the results for all five groups. The quantity Q is the deviation of the experimental angle average from $\bar{R}(0)$ in units of the expected standard deviation:

$$Q = \frac{[R(0)]_{\text{angle-average}} - \bar{R}(0)}{\{[\text{var}R(0)]/i\}^{1/2}}. \quad (5)$$

It is tempting to average Q over all five groups to characterize the over-all behavior. One finds that $Q_{\text{av}} = -0.05$, suggesting that on the average the fluctuations are well within expectation for $y=0$. However, the value of $Q = 3.81$ for $\alpha_2 + \alpha_3$ is highly improbable for a Gaussian distribution, which suggests that the $\alpha_2 + \alpha_3$

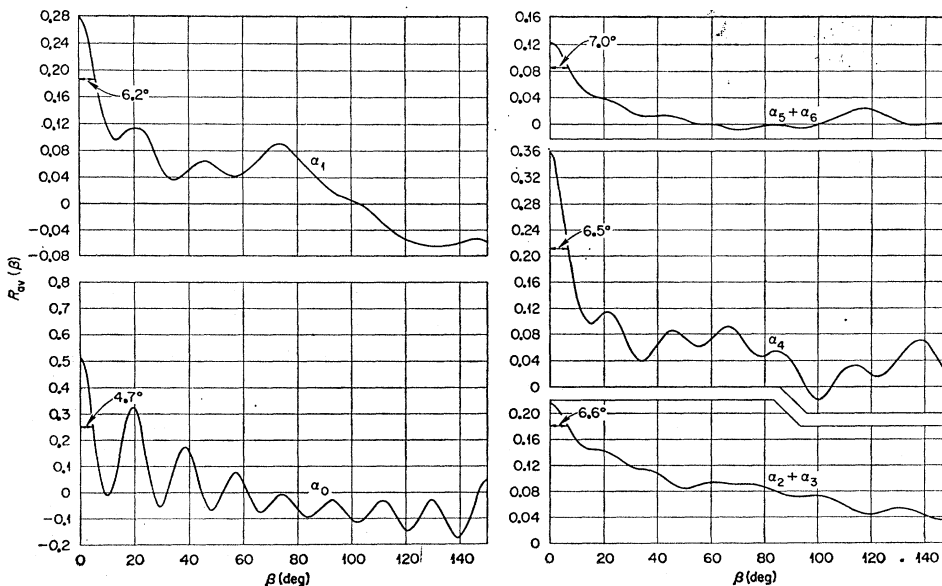


FIG. 14. Angle averages of the angular cross-correlation functions for the 31-MeV data.

data are not consistent with the statistical model adopted here.

C. $R(0)$ for Integrated Cross Sections

Ericson has pointed out¹⁵ that for angle-integrated cross sections the different partial waves add incoherently and the fluctuations are damped. The effective number N_{int} of independently fluctuating channels may be estimated by multiplying the number N of independent magnetic substates by the effective number of partial waves contributing. In this work we reverse this procedure and determine N_{int} by inversion of Eq. (B7) of Ref. 2, using the experimental values of $R(0)$ calculated from the integrated cross sections. The results are listed in Table III. In the last column they are divided by the estimated N values for the differential cross sections in order to obtain the damping factor (effective number of partial waves).

The angular-distribution analyses given earlier and the statistical-model calculations (Fig. 9) show that most of the cross section is provided by a few partial waves, perhaps four. The damping factors for α_1 , α_4 , and $\alpha_5 + \alpha_6$ are in agreement with this. The large damping for α_0 is not understood. The $\alpha_2 + \alpha_3$ group shows a much smaller effective number of partial waves.

It is possible to construct a class of statistical models more accurate than the one adopted here.¹⁶ Under some conditions these "R-matrix models" give rise to unusually strong, broad peaks dominated by one l -value.¹⁶ The $\alpha_2 + \alpha_3$ behavior seems to agree with qualitative predictions for these models,² but at present it is not possible to determine whether this behavior is quantitatively within normal limits for any model of this class.

D. Determination of Γ

The coherence width Γ of the participating compound states was obtained as a function of angle by two methods, from the width at half-maximum of the autocorrelation function³ and from the number of maxima per unit energy.⁴ The estimator $R(\epsilon)$ of the autocorrelation function given by Eq. (4) of Ref. 2 was used for this work. This function was calculated at each of the 64 different angles for α_0 , α_1 , and $\alpha_2 + \alpha_3$. Because of the small sample size, the result was frequently far from the expected Lorentzian. For example, the second

TABLE III. $R(0)$ for angle-integrated cross sections and N_{int} from inversion of Eq. (B7) of Ref. 2. The damping factor by which N_{int} is larger than the estimated N values of Table II is also shown.

Group	$R(0)$	N_{int}	Damping factor
α_0	0.0503	15.4	15.4
α_1	0.0647	11.9	4.0
$\alpha_2 + \alpha_3$	0.0965	7.9	1.0
α_4	0.0581	13.3	4.4
$\alpha_5 + \alpha_6$	0.0197	39.7	6.6

¹⁵ T. Ericson, Phys. Letters 4, 258 (1963).

¹⁶ P. A. Moldauer, Phys. Rev. Letters 18, 249 (1967).

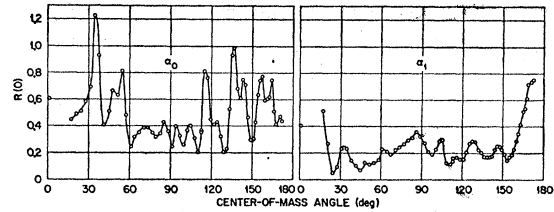


FIG. 15. Autocorrelation $R(0)$ as a function of angle for α_0 and α_1 in the 31-MeV region.

point of $R(\epsilon)$ was higher than $R(0)$ for about one-third of the angles. For consistency, it was decided to adhere to one objective criterion of width, namely, the value of ϵ for which $R(\epsilon)/R(0) = \frac{1}{2}$. The observed autocorrelation widths for α_0 , α_1 , and $\alpha_2 + \alpha_3$ are indicated by the full points connected by smooth curves in Fig. 16. Gaps in the curves correspond to the results which were clearly spurious, for example, those in which the second point of $R(\epsilon)$ is so small that it leads to widths smaller than the experimental energy resolution. Table IV lists the observed autocorrelation widths averaged over angle.

For excitation functions of finite length, the observed width is an underestimate of Γ . An approximate correction for the finite-sample bias is given in Appendix B of Ref. 2, Eq. (B13). In addition, a reduction of 3.8% in the observed autocorrelation width is necessary to correct for the 45-keV energy resolution [see Ref. 2, Eq. (5)]. The full points of Fig. 16 and the corrected autocorrelation results of Table IV incorporate these factors. The peak-counting results are indicated in Fig. 16 by the open circles; the b_N factor given in Appendix C of the previous paper² was used. The results are consistent with other determinations of Γ at this energy.^{1,2}

The averages over groups and corresponding standard deviations are also given in Table IV. The two methods of determining Γ give the same result within the statistical uncertainties. The standard deviation of differ-

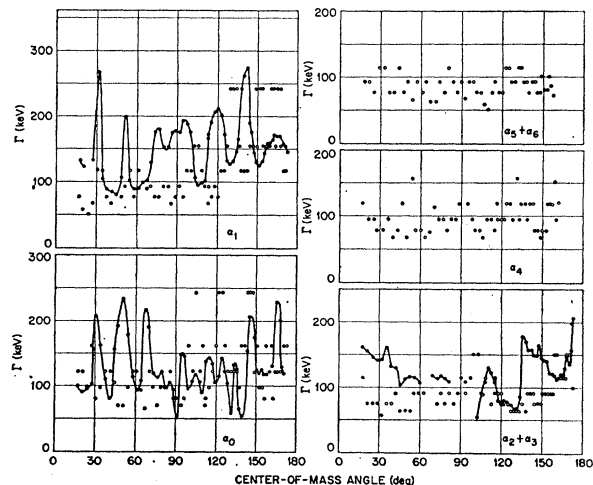


FIG. 16. Coherence widths in the 31-MeV region corrected for finite-sample effects, energy resolution, and spacing of experimental points. The full points are from the autocorrelation functions, while the open circles are the results from peak counting.

TABLE IV. Angle-averaged values and standard deviations of Γ in keV for the 31-MeV data. The corrected autocorrelation widths take account of energy-resolution and finite-sample effects. The widths from peak counting incorporate the tabulated values of b_N , which were taken from Appendix C of Ref. 2.

α group	Autocorrelation width		Width from peak counting	b_N
	Observed	Corrected		
α_0	94 ± 32	131 ± 45	133 ± 65	0.91
α_1	122 ± 35	154 ± 44	120 ± 56	0.90
$\alpha_2 + \alpha_3$	101 ± 26	124 ± 32	97 ± 28	0.88
α_4			100 ± 23	0.90
$\alpha_5 + \alpha_6$			90 ± 16	0.87
Average		136.3 ± 13.2	110.2 ± 17.9	

ent results for the same compound system is usually much smaller when Γ is determined by peak counting instead of from the autocorrelation function.^{2,17} For the present data, however, this does not appear to be true, possibly because the interval is short and the number of maxima, which of course must be an integer, is small. The over-all weighted average value of Γ is 125.2 ± 10.6 keV; the quoted uncertainty is merely the standard deviation of the average.

We now examine Fig. 16 for the dependence of Γ on angle. The autocorrelation widths are very similar over angle spans 5° to 10° wide. Other similarities in the structure of autocorrelation functions for neighboring angles also persist over angular intervals of this magnitude. These are in agreement with the coherence angles obtained in Sec. I. However, the average trend of the autocorrelation results of Fig. 16 shows little or no variation with angle. The same result is obtained with data over a wider range of energies.² The measured Γ is, in general, an average value over all Γ_J for compound states with different spin J . Since the high-spin states decay preferentially forward and backward,^{5,18} a strong dependence of Γ_J on J might be expected to show up as a variation with angle of the measured Γ .

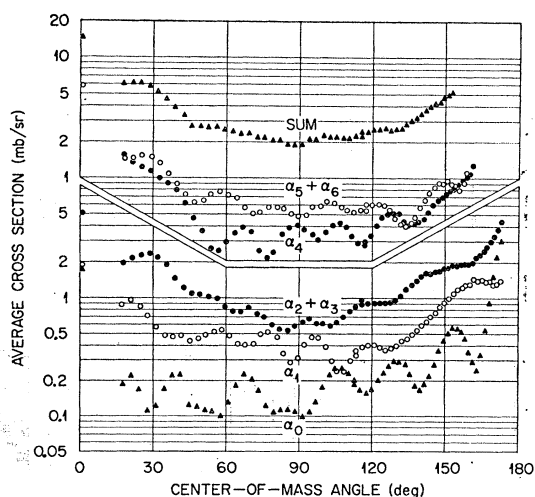


FIG. 17. Differential cross sections averaged over bombarding energies from 29.55 to 32.65 MeV. The uppermost curve is the sum over the five α -particle groups.

¹⁷ A. van der Woude, Nucl. Phys. **80**, 14 (1966).

¹⁸ T. Ericson and V. Strutinski, Nucl. Phys. **8**, 284 (1958); **9**, 689 (1958/59).

In the present case, however, a simplified estimate showed that the dominance of a few spin values near $J=10$ (seen in Fig. 9 for α_0) is sufficiently strong to overwhelm the contributions of the other compound states at all angles, and no angular variation of the average of Γ should be expected. As a corollary, the experimental coherence width gives Γ_{10} directly.

Measurements by Drysdale, Policarpo, and Phillips⁸ at 15° , 35° , and 55° covering the span of bombarding energy from 24.2 to 26.9 MeV (roughly 13Γ) show a decrease of the autocorrelation width with angle. In view of the large fluctuations of Γ with angle exemplified by the data of Fig. 16, there is no conflict with the present conclusion about the average trend of Γ .

The average trend of the peak-counting results for α_4 and $\alpha_5 + \alpha_6$ show the same insensitivity to angle as the autocorrelation results mentioned above. For the low-lying states, the increase with angle of the average Γ from peak counting conflicts with the autocorrelation results just discussed. The reason is unknown. It is worth noting, however, that the points with $\Gamma \approx 270$ keV correspond to excitation functions with only two maxima. Since the trend of Γ ought to be symmetric about 90° in any case, the peak-counting results for the low-lying states should be viewed with caution.

The excitation functions for the integrated cross sections (Fig. 10) also furnish estimates of Γ . The observed autocorrelation widths for α_0 and α_1 are 95 and 112 keV. The autocorrelation width for $\alpha_2 + \alpha_3$ is 206 keV, a result which may be typical not of the statistical fluctuations but rather of the broad peak which dominates the excitation function. The α_4 width is 64 keV, an unusually small value which conflicts with the angle-averaged value in Table IV. For $\alpha_5 + \alpha_6$, the lack of cross sections at back angles and resulting uncertainty in B_0 makes a reliable determination of Γ impossible.

V. ENERGY-AVERAGED CROSS SECTIONS

A. Differential Cross Sections

Figure 17 shows the experimental angular distributions averaged over the range of bombarding energies from 29.55 to 32.65 MeV. The slight variation in c.m. angle with energy was not taken into account here—the cross sections are actually averaged for fixed laboratory angle. Also shown is the sum of the average cross sections for the five α -particle groups.

The strong forward-backward peaking is due to the

dominance of high-spin compound states, and has been explained semiclassically by Ericson and Strutinski.^{5,18} According to the statistical model, the expectation value of the angular distributions is symmetric about 90° .^{5,19} The energy averaging damps the fluctuations and gives a result which may be compared with the expectation value. The general trend of the data is for symmetry about 90° . This is particularly evident in the sum, for which the fluctuations are the most highly damped. The detailed structure is asymmetric, but this is consistent with the expected residuum of fluctuations due to the finite length of the averaging interval. If we use (B5) of Ref. 2 to estimate the variance of the average cross section, then for $y=0$ we have $\text{RSD}(\sigma) = 0.46/\sqrt{N}$. It can be seen that in most cases the deviation from 90° symmetry falls within normal limits. For α_0 , however, the cross section beyond 90° tends to be two or three times larger than the forward cross section. This asymmetry seems to be too large to be accounted for by the expected $\text{RSD}(\sigma)$. Examination of the excitation functions from Ref. 2 may be useful here because they cover a wider range of energies and finite-sample effects are smaller. The 90° (c.m.) excitation-function data are in agreement with the expectation for $y=0$. Unfortunately, there is a gap in the excitation functions for the back angles just at these energies, so no further light can be shed on this matter.

B. Total Cross Sections

The averages of the angle-integrated cross sections near 31 MeV are given in Table V. The uncertainties tabulated are the expected $y=0$ standard deviations obtained from Eq. (B5) of Ref. 2 with N replaced by N_{int} from Table III; they do not include experimental error.

It is frequently stated that according to the statistical model the average cross sections should be proportional to the statistical weight of the level in question. The validity of this concept has been explored theoretically by MacDonald²⁰ and by a group at Saclay.¹² For this purpose the statistical weight is normally taken to be $(2j+1)$, where j is the spin of the final level, since there are $(2j+1)$ magnetic substates. Except for α_0 , the integrated cross sections are nearly proportional to $(2j+1)$, as shown in Table V. However, for consistency with the fluctuation analyses adopted in this paper one should perhaps choose a statistical weight equal to N since it was assumed that the N channels contribute equally. As shown in Table V, this choice gives reasonably good proportionality to the statistical weight for all groups.

VI. SUMMARY AND CONCLUSIONS

Detailed angular distributions for $^{12}\text{C}(^{16}\text{O}, \alpha)^{24}\text{Mg}$ were measured at closely spaced energy intervals in four regions of bombarding energy. The increase in angular momentum with energy is clearly shown by the increas-

TABLE V. Angle-integrated cross sections in mb averaged over bombarding energies from 29.55 to 32.65 MeV. Also given are the cross sections divided by two choices for the statistical weight. The quoted uncertainties come from the expected standard deviations.

Group	σ_T	$\sigma_T/(2j+1)$	σ_T/N
α_0	2.87 ± 0.34	2.87 ± 0.34	2.87 ± 0.34
α_1	6.42 ± 0.50	1.28 ± 0.10	2.14 ± 0.17
$\alpha_2 + \alpha_3$	13.85 ± 0.80	0.99 ± 0.06	1.73 ± 0.10
α_4	6.21 ± 0.46	1.04 ± 0.08	2.07 ± 0.15
$\alpha_5 + \alpha_6$	9.39 ± 0.28	0.94 ± 0.03	1.57 ± 0.05

ing complexity of the angular distributions. Near 31 MeV (~ 30 -MeV excitation energy in the ^{28}Si compound nucleus) the dominant compound states are those with $J \sim 10$.

Analyses of the fluctuations in these data revealed the following. (a) The coherence angle is about 6.2° , in good agreement with the expected value. (b) The average coherence energy Γ is about 125 keV and does not depend on angle because of the dominance of a few angular momenta. (c) Measurements with 15-keV resolution revealed no structure finer than 100 keV. (d) The data are generally consistent with the hypothesis that the nonfluctuating (direct-interaction) component of the cross section is zero. (e) The $\alpha_2 + \alpha_3$ data are not consistent with the predictions of the Ericson and Brink-Stephen model. The differential cross section shows too much fluctuation, and the fluctuations in the angle-integrated cross section are damped much less than expected. However, the $\alpha_2 + \alpha_3$ behavior may be within normal limits of a more accurate model.

Averaging the differential cross sections over energy damps the fluctuations and tends to give 90° symmetry, in accordance with expectation from the statistical model. Strong forward-backward peaking occurs because of the high angular momentum involved. The angle-integrated average cross sections are approximately proportional to the statistical weights of the various final levels of ^{24}Mg .

Except possibly for the unusual $\alpha_2 + \alpha_3$ behavior, there is over-all agreement with the statistical model, and this reaction may be characterized as a predominantly compound-nucleus process.

ACKNOWLEDGMENTS

We wish to thank the operators of the tandem accelerator under G. F. Wells for their helpful cooperation. H. F. Bowsher assisted us greatly by making the carbon targets. We received help in accumulating and processing the data from many individuals, principally L. C. Becker, C. R. Bingham, H. F. Bowsher, I. M. Brann, C. H. Johnson, G. A. Palmer, and T. P. Whaley. Discussions and correspondence with M. Böhning, A. van der Woude, J. A. Kuehner, and the late E. Almqvist were especially helpful. We should also like to thank E. Vogt and D. McPherson for the statistical-model calculations, and E. C. Halbert, W. R. Gibbs, and R. B. Leachman for their careful reading of the manuscript.

¹⁹ L. Wolfenstein, Phys. Rev. **82**, 690 (1951).

²⁰ N. MacDonald, Nucl. Phys. **33**, 110 (1963).

²¹ L. Papineau, Saclay Report No. CEA-R2876 (unpublished).